Magnetic behavior of nanocrystalline $ErCo_2$

2009 J. Phys.: Condens. Matter 21 296004

(http://iopscience.iop.org/0953-8984/21/29/296004)

J. Phys.: Condens. Matter **21** (2009) 296004 (5pp) doi:10.1088/0953-8984/21/29/296004

Magnetic behavior of nanocrystalline $ErCo_2$

Sitikantha D Das, Niharika Mohapatra, Kartik K Iyer, R D Bapat and E V Sampathkumaran

Tata Institute of Fundamental Research, Homi Bhabha Road, Colaba, Mumbai 400005, India

E-mail: sampath@mailhost.tifr.res.in

Received 3 March 2009
Published 3 July 2009
Online at stacks.iop.org/JPhysCM/21/296004

Abstract

We have investigated the magnetic behavior of the nanocrystalline form of a well-known Laves phase compound, $ErCo_2$—the bulk form of which has been known to undergo an interesting first-order ferrimagnetic ordering near 32 K—synthesized by high-energy ball-milling. It is found that, in these nanocrystallites, Co exhibits ferromagnetic order at room temperature, as inferred from the magnetization data. However, the magnetic transition temperature for the Er sub-lattice remains essentially unaffected suggesting the (Er)4f–Co(3d) coupling is weak on Er magnetism. The net magnetic moment as measured at high fields, for example at 120 kOe, is significantly reduced with respect to that for the bulk in the ferrimagnetically ordered state and possible reasons are outlined for this. We have also compared the magnetocaloric behavior for the bulk and for nanoparticles.

(Some figures in this article are in colour only in the electronic version)

1. Introduction

Laves phase compounds, RCo_2 (R = Rare-earths), have attracted considerable attention in the literature during the last few decades, as this family serves as a model system for itinerant electron metamagnetism (IEM) [1]. For instance, YCo_2 and $LuCo_2$, the exchange-enhanced Pauli-paramagnets, have been found to undergo IEM at about 700 kOe [2, 3]. With respect to those members in which R carries a localized-moment, quite interestingly, the magnetic transition appears to be first order for R = Dy, Ho, and Er, whereas for many other members of this series, it is second order. It is generally accepted that the first-order nature of the transition for the former members is due to the onset of IEM at the Co site induced by the molecular field arising from the magnetic ordering of the R sub-lattice. This finding has led to intense investigations [4], particularly with respect to potential magnetic refrigeration applications [5].

While all the reports on these heavy rare-earth members is on the bulk form (single crystals and polycrystals), very little work has been carried out on the nanocrystalline form, as it is not usually easy to stabilize nanoparticles of rare-earth intermetallics without shell protection. In this respect, there is a recent claim on the synthesis of oxidation-resistant $DyCo_2$ nanoparticles by an arc-discharge process [6] with promising low-temperature refrigeration applications. In this paper, we present the results of our magnetic investigation on the nanoparticles of $ErCo_2$ synthesized by high-energy ball-milling[1], the reason being that this compound in particular has attracted considerable attention in the recent literature [8–20, 22]. This compound has been found to order ferrimagnetically at (T_C=) 32 K due to the antiparallel alignment of Er and Co moments (with a moment on Co being about 1 μ_B) [8] with an extreme sensitivity of T_C to small amounts of metallic impurity [9, 10]. This compound has been extensively studied for its magnetocaloric effect (MCE) [11–13]. The so-called 'inverse IEM' phenomenon has been noted for some degree of chemical doping [20].

2. Experimental details

The bulk sample was prepared by arc melting stoichiometric amounts of high-purity (>99.9%) constituent elements in an atmosphere of argon. The molten ingot was annealed at 900 °C for 60 h in an evacuated sealed quartz tube. The ingot was then subjected to high-energy ball-milling (Fritsch pulverisette-7 premium line) for $2\frac{1}{2}$ h employing zirconia vials

[1] Through this procedure, in the past, we were able synthesize a stable form of nanoparticles of YCo_2, with ferromagnetism at room temperature. See [7].

with balls of 5 mm diameter (ball-to-material mass ratio: 5) with an operating speed of 500 rpm in an atmosphere of toluene. The specimens were characterized by x-ray diffraction (XRD), scanning electron microscope (SEM, JEOL, JSM 840A), transmission electron microscope (TEM, Technai 200 kV) and energy-dispersive x-ray analysis. A commercial magnetometer (Quantum Design) was employed to measure the magnetization.

3. Results and discussion

The XRD patterns are shown in figure 1 for both the ingot and milled specimens. The patterns are shifted along the y-axis for the sake of clarity. Otherwise the background intensity and shape of the background are found to be essentially the same for both the specimens, thereby indicating that milling does not result in amorphous formation. The sharp XRD lines additionally confirm that the milled samples are crystalline. We did not find any noticeable change in the lattice constants (as determined from XRD) due to ball-milling. As is well known in the field of metallurgy, milling reduces the intensity of the XRD lines. The XRD lines are broadened as demonstrated in an inset of figure 1 and the average particle size, if estimated from the width of the most intense line, turns out to be about 30 nm. The nanosized nature of the specimen was ascertained from TEM pictures (see figure 1). However, the TEM picture suggests that the particle size is smaller than that estimated from XRD. We attribute this discrepancy to the fact that the strain-contribution to the broadening of the XRD lines could not be separated due to non-linear Williamson–Hall plots (not shown here). The electron diffraction pattern inserted in figure 1 confirms that the particles belong to the $ErCo_2$ phase. We have also carried out Rietveld fitting of the XRD pattern for the milled specimen, and the difference between the experimental and fitted pattern is shown in figure 1 to exhibit proper phase formation. There is no evidence in the XRD for the formation of any other phase due to ball-milling. From the backscattered image of the SEM, we further confirmed the absence of any other phase in the nanospecimen. In addition, the stoichiometry of the nanospecimen was established to correspond to $ErCo_2$ from energy-dispersive x-ray analysis performed with this SEM instrument.

The results of magnetization measurements as a function of temperature (T) and magnetic field (H) for the zero-field-cooled (ZFC from 300 K) and field-cooled (FC) conditions of the milled specimen are shown in figures 2 and 3 respectively. The data obtained on the parent ingot is also included for comparison. In the ingot employed to prepare the fine particle, we see the features attributable to the onset of magnetic ordering near 36 K as inferred, for example, from the peak temperature in the $M(T)$ obtained in a field of 100 Oe. It is straightforward to see the changes (see figure 2) that have occurred in the shapes of $M(T)$ curves after milling. Most notably, the sharpness of the features seen at T_C for the bulk specimen is absent for the nanoparticles; see, for instance, the features in the ZFC curve ($H = 100$ Oe). This is attributable to the broadening of the magnetic transition due to defects introduced by ball-milling. In addition to the above

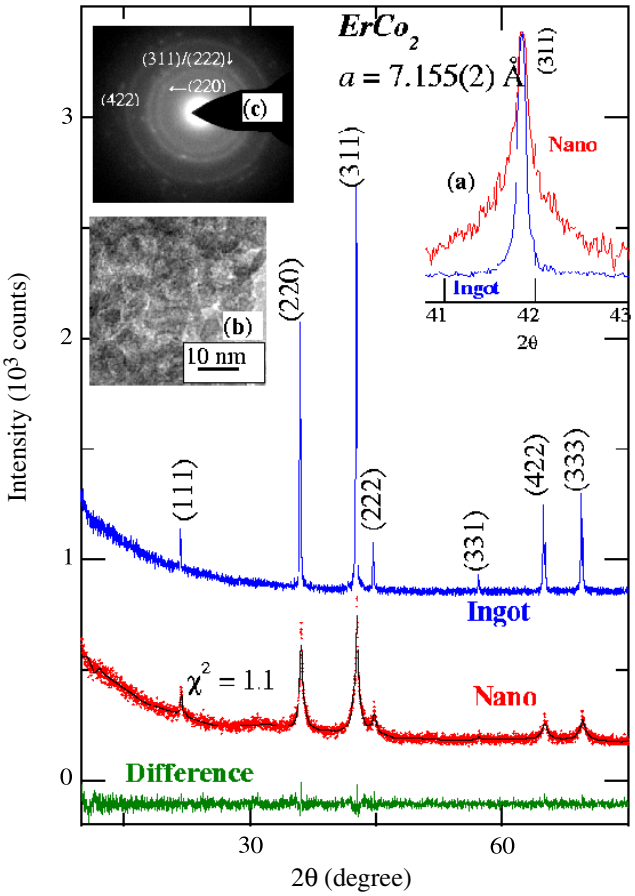

Figure 1. X-ray diffraction patterns of the bulk and nanocrystals of $ErCo_2$. The fit obtained by Rietveld analysis in the case of the nanospecimen is shown by the continuous line and the difference between the fit and the experimental data points is also shown. In inset (a), the shapes of the most intense lines are compared after normalizing to respective peak heights. In insets (b) and (c), the TEM image and electron diffraction pattern are shown.

features near the magnetic transition temperature, there is a bifurcation of the ZFC–FC curves extending beyond 36 K in the nanospecimen, which is indicative of another magnetic anomaly at higher temperatures. This aspect is addressed in the next paragraph on the basis of the $M(H)$ anomaly.

For the bulk specimen, the $M(H)$ plots (figure 3) are hysteretic below 20 kOe in the magnetically ordered state and the value of M tends towards saturation beyond 30 kOe with the saturation moment (for example, about 7.2 μ_B/f.u. at 1.8 K, see also [13]) being less than that expected for trivalent Er ions due to ferrimagnetism. As expected, in the paramagnetic state, for example, at 50 K, the plot of $M(H)$ is linear. On the other hand, in the nanoform, the hysteretic nature of the curve persists even near 50 kOe, for instance, at 1.8 and 30 K (see figure 3) without any evidence for saturation; in addition, the high-field magnetic moment is significantly reduced. On the basis of these $M(H)$ properties, we infer that ferrimagnetism is retained in the nanoform. If one performs a linear extrapolation of the high-field data to zero field at 1.8 K, assuming that the moment on Er is unchanged, we arrive at a value of at least 2 μ_B on each Co ion for the

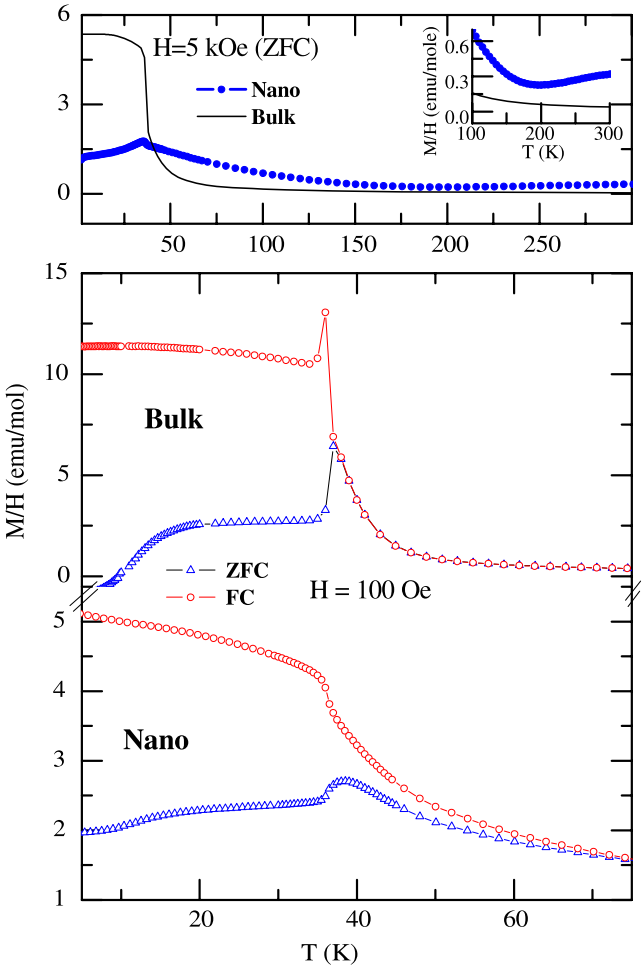

Figure 2. Magnetization (M) divided by magnetic field (H) as a function of temperature (T) for the bulk and for nanocrystals of $ErCo_2$ for two values of externally applied magnetic fields. In the case of $H = 100$ Oe, the curves for the zero-field-cooled and field-cooled conditions of the nanoparticles are shown. The lines through the data points serve as guides to the eyes. The inset highlights the increasing M/H behavior above 200 K for the nanocrystals (shown along with the data for the bulk).

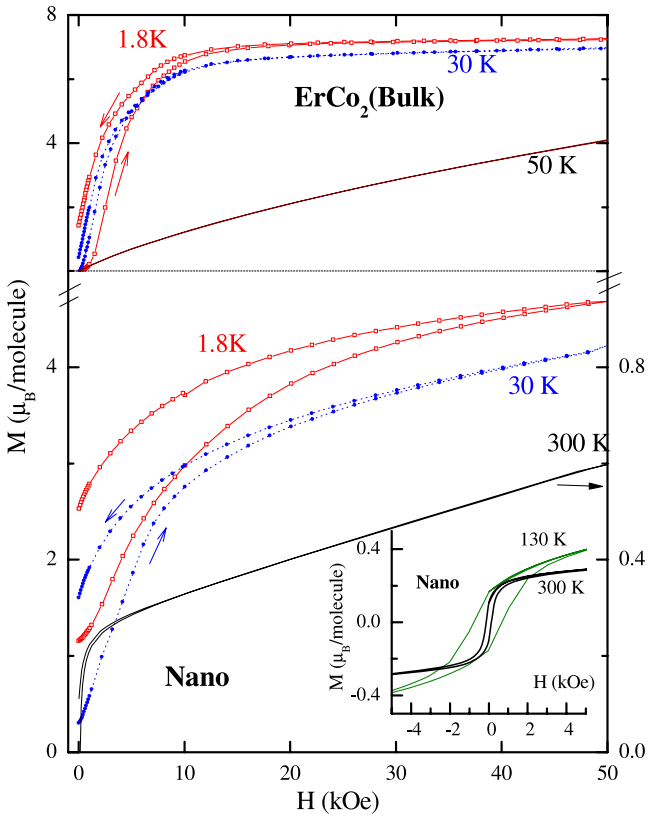

Figure 3. Isothermal remnant behavior at selected temperatures for the bulk and for nanocrystals of $ErCo_2$. The lines through the data points serve as guides to the eyes. In the inset, low-field hysteresis loops at 130 and 300 K for the nanocrystals are plotted.

nanoform. Thus, if one solely attributes the observed reduction of the high-field magnetic moment to Co, then there is an enhancement in the magnetic moment on Co following Er sub-lattice ordering. However, it is also possible that a significant surface spin disorder due to lack of symmetry and reduced coordination at the surface is also responsible for the observed behavior, as known, for instance, for the nanoform of γ-Fe_2O_3 [22]. The finding we stress for the nanoform is that, well above 36 K, the $M(H)$ plots show a dramatic increase for initial applications of magnetic field with a linearity at higher fields, suggesting there is a ferromagnetic component superimposed over a paramagnetic component. The plots are hysteretic at low fields as shown for 130 and 300 K in the inset of figure 3. These findings reveal that Co in the nanoparticle exhibits a ferromagnetic character at room temperature with Er remaining paramagnetic. The value of the magnetic moment on Co turns out to be $\sim 0.12\mu_B$/Co, at least above 32 K. We believe that when Er is paramagnetic, it is possible that Co spins undergo a 'canted' ferromagnetic alignment, as the magnetic moment value is lower than that observed [7] in YCo_2. In support of a complex magnetic ordering of Co, the plot of M/H exhibits an increase above 200 K, as shown in the inset of figure 2. It would be of interest to carry out neutron diffraction studies to understand this issue better. In any case, it is clear that there is a magnetic ordering of Co in the nanoparticles of $ErCo_2$ above room temperature. It is to be stressed that, despite the high magnetic ordering temperature of Co, the T_C for the Er sub-lattice is not noticeably influenced.

We find dramatic modifications of Arrott plots in the temperature range where the Er sub-lattice undergoes magnetic ordering (see figure 4). For the ingot, these plots have been known to be complex, with negative slopes and inflexions due to metamagnetic transitions, the exact nature of which appears to be sample dependent (see, for instance, [13, 21]). In the nanospecimen, though M^2 increases monotonically with H/M, the plot is still complex, which is attributable to a possible interference from Co sub-lattice ordering at higher temperatures.

We compare MCE properties in figure 5 for a typical change of magnetic field. For this purpose, we in fact obtained $M(H)$ curves at close intervals of temperatures and derived the entropy change, ΔS, for a given variation of H (from zero field), on the basis of the well-known Maxwell's relation (see, for instance, [5]). The results are shown

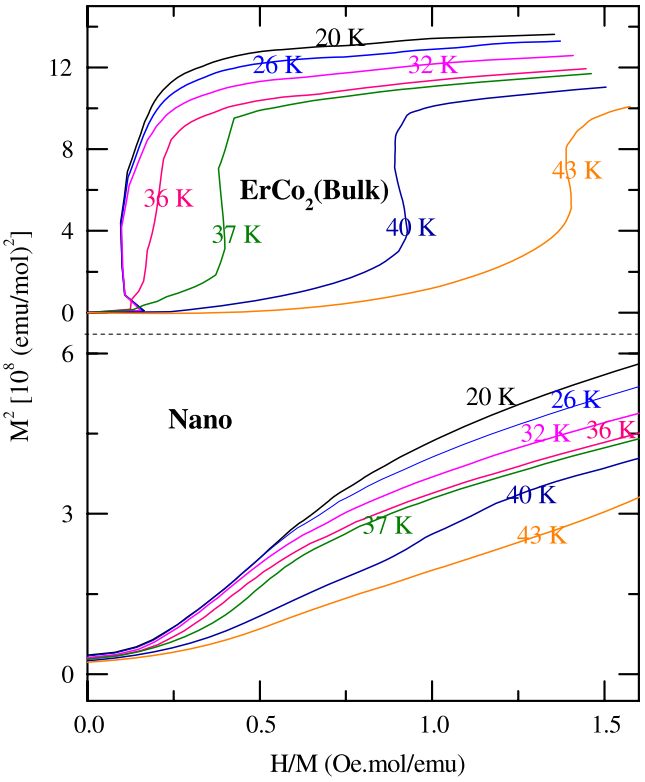

Figure 4. The Arrott plots for bulk and nanocrystals of $ErCo_2$. For the sake of clarity, we show only the lines through the data points.

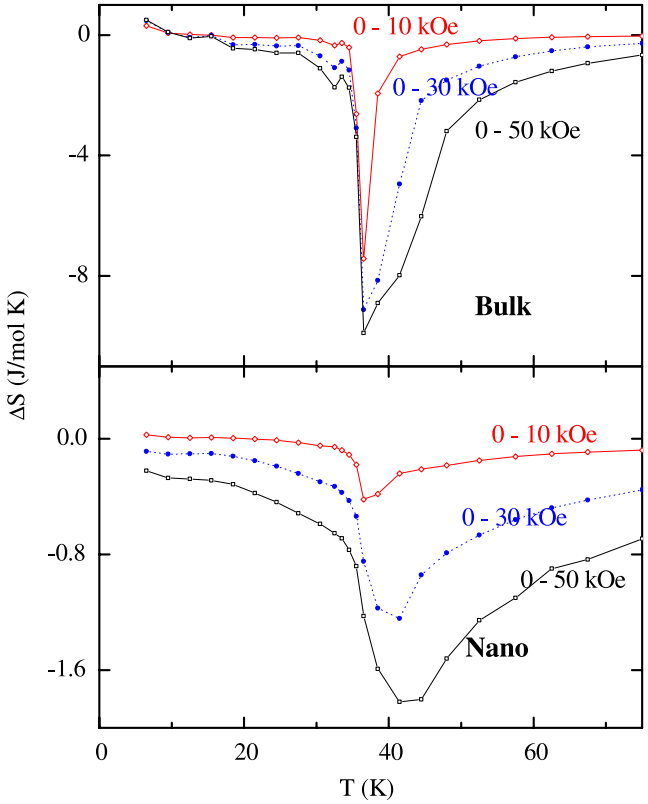

Figure 5. The temperature dependence of entropy change for different variations of magnetic fields for the bulk and for nanocrystals of $ErCo_2$. The lines through the points serve as guides to the eyes.

in the figure for selected fields. The results obtained for the ingot are in good agreement with those known in the literature [11–13, 21]. It is distinctly clear from figure 5 that, in the case of the nanospecimen, though ΔS values at the peak are relatively reduced at T_C, the curve broadly extends over a wider temperature range. The magnetic refrigeration capacity (for the definition we use, see [23]), turns out to be about half that seen for the bulk form (about 80 J mol^{-1}).

4. Conclusion

The compound, $ErCo_2$, has attracted attention in the literature from the viewpoint of its potential magnetic refrigeration applications as well as of its interesting magnetic anomalies. We have synthesized nanocrystals of this material, to our knowledge, for the first time and studied its magnetic behavior. The Co sub-lattice is found to be magnetically ordered at room temperature in these fine particles; unlike in the bulk. It is notable that the transition temperature for the Er sub-lattice is not influenced at all by the high-temperature magnetism of the Co sub-lattice, suggesting Er–Co magnetic coupling is weak in the nanoform. There is a significant reduction in the high-field magnetic moment compared to that of the bulk when the Er sub-lattice orders at low temperatures. Although the magnetic refrigeration capacity becomes half that of the bulk material in the temperature range of interest, the entropy change is spread over a rather larger temperature range when compared to that in the bulk form.

This family of binary compounds are characterized by a sharp density of the 3d states of Co in the vicinity of the Fermi level and, in the case of pseudo-binary compounds based on YCo_2, even defects have been proposed as having a profound effect on this feature and hence on magnetism [24]. It is not clear whether a similar effect is responsible for the magnetism of Co in the ball-milled $ErCo_2$ as well. Thus, it appears that this family could be a good example for probing the interplay between the defects, electronic structure and strong electron correlations.

References

[1] Wohlfarth E P and Rhodes P 1962 *Phil. Mag.* **7** 1817
[2] Goto T, Fukamichi K, Sakakibara T and Komatsu H 1989 *Solid State Commun.* **72** 945
[3] Yamada H, Tohyama T and Shimizu M 1987 *J. Magn. Magn. Mater.* **70** 44
Yokoyama T *et al* 2001 *J. Phys.: Condens. Matter* **13** 9281
[4] Khmelevskyi S and Mohn P 2000 *J. Phys.: Condens. Matter* **12** 9453
Duc N H and Goto T 1999 *Handbook on the Physics and Chemistry of Rare Earths* vol 28, ed K A Gschneidner Jr and L Eyring (Amsterdam: North-Holland) p 177 and references therein
[5] See, for a review Gschneidner K A Jr, Pecharsky V K and Tsokol A O 2005 *Rep. Prog. Phys.* **68** 1479
[6] Ma S, Cui W B, Li D, Sun N K, Geng D Y, Jiang X and Zhang Z D 2008 *Appl. Phys. Lett.* **92** 173113
[7] Narayana Jammalamadaka S, Sampathkumaran E V, Satya Narayana Murthy V and Markandeyulu G 2008 *Appl. Phys. Lett.* **92** 192506

[8] Moon M, Koehler W C and Farrell J 1965 *J. Appl. Phys.* **36** 978
[9] Liu X B and Altounian Z 2008 *J. Appl. Phys.* **103** 07B304
[10] Guillot M and Öner Y 2008 *J. Appl. Phys.* **103** 07E137
[11] Cuong T D, Havela L, Sechovsky V, Andreev A V, Amold Z, Kamarad J and Duc N H 1997 *J. Appl. Phys.* **81** 4221
[12] Wada H, Tomekawa S and Shiga M 1999 *Cryogenics* **39** 915
[13] Gigurre A, Foldeaki M, Schnelle W and Gmelin E 1999 *J. Phys.: Condens. Matter* **11** 6969
[14] Herrero-Albillos J, Paudyal D, Bartolome F, Garcia L M, Pecharsky V K, Gschneidner K A Jr, Young A T, Jaouen N and Rogalev A 2008 *J. Appl. Phys.* **103** 07E146
[15] Ishimatsu N, Miyamoto S, Maruyama H, Chaboy J, Laguna-Marco M A and Kawamura N 2007 *Phys. Rev.* B **75** 180402(R)
[16] Syshchenko O, Sechovsky V, Divis M, Fujita T, Hauser R and Fujii H 2001 *J. Appl. Phys.* **89** 7323
[17] Syschenko O, Fujita T, Sechovsky V, Divis M and Fujii H 2001 *Phys. Rev.* B **63** 054433
[18] Hauser R, Bauer E and Gratz E 1998 *Phys. Rev.* B **57** 2904
[19] Podlesnyak A, Strässle Th, Schefer J, Furrer A, Mirmelstein A, Pirogov A, Markin P and Baranov N 2002 *Phys. Rev.* B **66** 012409
[20] Hauser R, Bauer E, Gratz E, Mueller H, Rotter M, Michor H, Hilscher G, Markosyan A S, Kamishima K and Goto T 2000 *Phys. Rev.* B **61** 1198
[21] Zou J-D, Shen B-G and Sun J-R 2007 *Chin. Phys.* **16** 1817
[22] Shendruk T N, Desautels R D, Southern B W and van Lierop J 2007 *Nanotechnology* **18** 455704
Tronc E, Fiorani D, Nogues M, Testa A M, Lucari F, D'Orazio F, Greneche J M, Wernsdorfer W, Galvez N, Chaneac C, Mailly D and Jolivet J P 2003 *J. Magn. Magn. Mater.* **262** 6
[23] Mohapatra N, Iyer K K and Sampathkumaran E V 2008 *Eur. Phys. J.* B **63** 451
[24] Burkov A T, Bauer E, Gratz E, Resel R, Nakama T and Yagasaki K 2008 *Phys. Rev.* B **78** 035101